$G_{q/11}$-dependent regulation of endosomal cAMP generation by parathyroid hormone class B GPCR

Alex D. White[a,b,1], Frederic G. Jean-Alphonse[a,1,2], Fei Fang[a], Karina A. Peña[a], Shi Liu[c], Gabriele M. König[d], Asuka Inoue[e], Despoina Aslanoglou[f], Samuel H. Gellman[c], Evi Kostenis[d], Kunhong Xiao[a], and Jean-Pierre Vilardaga[a,3]

[a]Department of Pharmacology and Chemical Biology, School of Medicine, University of Pittsburgh, Pittsburgh, PA 15261; [b]Graduate Program in Molecular Pharmacology, School of Medicine, University of Pittsburgh, Pittsburgh, PA 15261; [c]Department of Chemistry, University of Wisconsin–Madison, WI 53706; [d]Molecular, Cellular and Pharmacobiology Section, Institute of Pharmaceutical Biology, University of Bonn, 53115 Bonn, Germany; [e]Graduate School of Pharmaceutical Sciences, Tohoku University, 980-8578 Sendai, Miyagi, Japan; and [f]Department of Psychiatry, School of Medicine, University of Pittsburgh, Pittsburgh, PA 15261

Edited by Robert J. Lefkowitz, Howard Hughes Medical Institute, Durham, NC, and approved February 18, 2020 (received for review October 16, 2019)

cAMP production upon activation of G_s by G protein-coupled receptors has classically been considered to be plasma membrane-delimited, but a shift in this paradigm has occurred in recent years with the identification of several receptors that continue to signal from early endosomes after internalization. The molecular mechanisms regulating this aspect of signaling remain incompletely understood. Here, we investigated the role of $G_{q/11}$ activation by the parathyroid hormone (PTH) type 1 receptor (PTHR) in mediating endosomal cAMP responses. Inhibition of $G_{q/11}$ signaling by FR900359 markedly reduced the duration of PTH-induced cAMP production, and this effect was mimicked in cells lacking endogenous $G\alpha_{q/11}$. We determined that modulation of cAMP generation by $G_{q/11}$ occurs at the level of the heterotrimeric G protein via liberation of cell surface Gβγ subunits, which, in turn, act in a phosphoinositide-3 kinase-dependent manner to promote the assembly of PTHR–βarrestin–Gβγ signaling complexes that mediate endosomal cAMP responses. These results unveil insights into the spatiotemporal regulation of G_s-dependent cAMP signaling.

GPCR | endosomal signaling | PTH | G-proteins | cAMP

The parathyroid hormone (PTH) type 1 receptor (PTHR) is a class B G protein-coupled receptor (GPCR) that mediates the biological effects of endogenous peptide ligands PTH and PTH-related peptide (PTHrP) (1). Although the receptor functions to regulate growth and development of various tissues in response to PTHrP, PTH-induced activation of the PTHR serves a critical role in homeostatic control of systemic Ca^{2+} and phosphate levels, as well as bone remodeling (2). Although both ligands exert their physiological effects via binding to the same receptor and subsequent activation of G_s/cAMP and G_q/Ca^{2+} signaling pathways (3), PTH and PTHrP are distinguished by cAMP responses that differ markedly in duration and cellular localization (4, 5). Association of PTHrP with the receptor permits only transient cAMP production from the cell membrane that is consistent with the classical model of GPCR signaling (5). The receptor is also capable of promoting sustained cAMP generation after internalization of highly stable PTH–PTHR complexes that remain active in early endosomes (4). Furthermore, accumulating evidence suggests that these differential modes of signaling may give rise to distinct biological outcomes. For example, a recently identified point mutation in PTH (Arg25 → Cys) that abolishes endosomal signaling causes severe hypocalcemia in patients harboring this mutation (6, 7). In agreement with this finding, injection of a long-acting PTH (LA-PTH) analog into mice causes prolonged hypercalcemic responses that correlate with the propensity to promote sustained cAMP from endosomes (8). Despite significant advancements in identifying the physiological relevance of PTHR endosomal signaling (5, 9), its underlying molecular mechanisms and regulation remain incompletely understood. We recently reported on the development of G_s-biased PTH analogs that stimulate cAMP production but fail to engage in endosomal cAMP signaling due to impaired recruitment of βarrestins (βarrs) (10). Observation that these same ligands also show deficient G_q signaling, as measured by reduced intracellular Ca^{2+} mobilization in HEK293 cells stably expressing PTHR (HEK-PTHR), led us to question whether G_q signaling serves as a regulator of PTHR-mediated endosomal cAMP responses.

Results

In support of this hypothesis, the selective $G_{q/11}$ inhibitor FR900359 markedly decreased the duration of PTH-induced cAMP responses in HEK-PTHR cells (Fig. 1*A* and *SI Appendix*, Fig. S1*A*), and this effect was recapitulated in bone and kidney cells endogenously expressing the receptor (Fig. 1 *B–D* and *SI Appendix*, Fig. S1 *B–D*). FR900359 efficacy was confirmed by its ability to block PTH activation of heterotrimeric G_q proteins (*SI Appendix*, Fig. S2*A*),

Significance

Binding of parathyroid hormone (PTH) to its cognate receptor (PTHR) has been shown to induce prolonged cAMP responses from early endosomes. While the receptor also couples to $G_{q/11}$, whether this pathway modulates sustained cAMP remains unexplored. Here, we show that lack of $G_{q/11}$ activation reduces the duration of PTH-induced cAMP generation. Our findings reveal that this effect occurs at the level of the G protein, rather than downstream effectors, via provision of Gβγ subunits at the cell surface. We demonstrate that $G_{q/11}$-derived Gβγ subunits act in a phosphoinositide-3 kinase-dependent manner to promote assembly of ternary PTHR–βarrestin–Gβγ complexes that are required for PTH-mediated sustained cAMP from endosomes. These findings provide insights into the spatiotemporal regulation of GPCR signaling.

Author contributions: J.-P.V. designed research; A.D.W., F.G.J.-A., F.F., K.A.P., and K.X. performed research; S.L., G.M.K., A.I., D.A., S.H.G., and E.K. contributed new reagents/analytic tools; A.D.W., F.G.J.-A., and J.-P.V. analyzed data; and A.D.W. and J.-P.V. wrote the paper.

The authors declare no competing interest.

This article is a PNAS Direct Submission.

Data deposition: MS data have been deposited into MassIVE and are accessible upon request from authors.

[1]A.D.W. and F.G.J.-A. contributed equally to this work.

[2]Present address: Unité de la Physiologie de la Reproduction et des Comportements, Institut National de Recherche pour l'Agriculture, l'Alimentation et l'Environnement (INRAE), CNRS, 37380 Nouzilly, France.

[3]To whom correspondence may be addressed. Email: jpv@pitt.edu.

This article contains supporting information online at https://www.pnas.org/lookup/suppl/doi:10.1073/pnas.1918158117/-/DCSupplemental.

First published March 17, 2020.

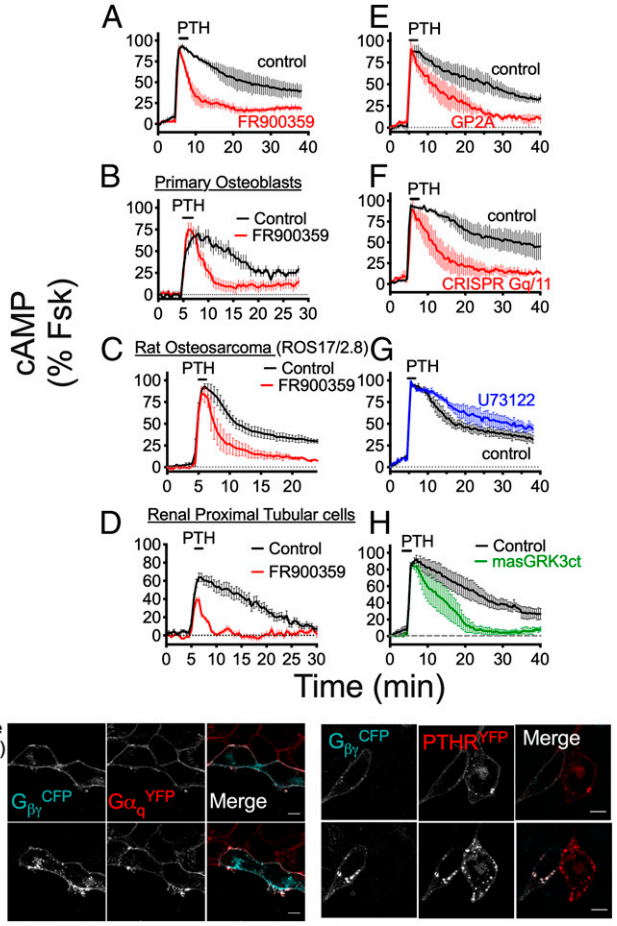

Fig. 1. $G_{q/11}$-dependent cAMP production by PTH. (*A*) Time courses of cAMP production recorded by FRET in response to 10 nM PTH in single HEK-PTHR cells ±FR900359. (*B–D*) Similar assay as in *A* in response to 100 nM PTH in primary osteoblasts isolated from mice (*B*), rat osteosarcoma (ROS)17/2.8 cells (*C*), and renal proximal tubular epithelial cells (RPTEC) (*D*). (*E–H*) Similar as in *A* ±GP2A (*E*), in parental and HEK-$G_{q/11}^{KO}$ cells (*F*), and as in *A* with the PLC inhibitor U73122 (*G*), or in the absence (control) or presence of the masGRK3ct (*H*). cAMP data represent mean values ± SEM of n = 3–4 independent experiments and n = 15–45 cells per experiment for *A*, *C*, *E*, *F*, and *G*, and n = 16–25 cells for 1 experiment for *B* and *D*. See *SI Appendix*, Fig. S1 for statistical analyses. (*I*) Fluorescence micrographs corresponding to the individual and merged channel data of HEK cells cotransfected with $G\beta\gamma^{CFP}$ (cyan) and either $G\alpha_q^{YFP}$ or $PTHR^{YFP}$ (red). Images were recorded at 30-s intervals for 15 min after a brief challenge with 100 nM PTH. (Scale bars: 10 μm.)

measured by changes in FRET of the $G_q^{CFP/YFP}$ sensor, as well as the release of Ca^{2+} from intracellular ER stores (*SI Appendix*, Fig. S2*B*). Similar effects were observed on cAMP generation, using another $G_{q/11}$ inhibitor, GP2A (Fig. 1*E* and *SI Appendix*, Fig. S1*E*), as well as in HEK293 cells lacking endogenous $G\alpha_{q/11}$ (HEK-$G_{q/11}^{KO}$; Fig. 1*F* and *SI Appendix*, Figs. S1*F* and S3 *A–C*). Saturation and competition binding experiments at equilibrium using intact live cells revealed that impaired cAMP signaling in HEK-$G_{q/11}^{KO}$ cells was not due to changes in PTH binding affinity (*SI Appendix*, Fig. S3 *D* and *E*), indicating that $G_{q/11}$-mediated effects on cAMP responses likely occur after ligand association with the receptor. Inhibition of the $G_{q/11}$ downstream effector PLC by U73122 had no effect on PTH-induced cAMP (Fig. 1*G* and *SI Appendix*, Fig. S1*G*); thus, these results collectively demonstrate that $G_{q/11}$ activation, as opposed to PLC-dependent signaling, is determinant for endosomal PTHR cAMP generation.

To delineate the roles of Gα and Gβγ subunits in $G_{q/11}$-mediated regulation of cAMP, we next used live-cell confocal microscopy to monitor the localization of fluorescently labeled G protein subunits. Under basal conditions, both $G\alpha_q^{YFP}$ and $G\beta\gamma^{CFP}$ were observed primarily at the plasma membrane, along with a small fraction located in subcellular compartments (Fig. 1*I*; t = 0 min); however, brief stimulation with PTH induced significant translocation of Gβγ intracellularly that colocalized with the receptor, while $G\alpha_q$ remained at the cell surface (Fig. 1*I*; t = 15 min). Subsequent cAMP time-course experiments revealed that translocation of Gβγ originating from the cell surface is critical for endosomal signaling, as expression of masGRK3ct, a Gβγ scavenger that localizes exclusively to the plasma membrane (11), completely abolished sustained signaling induced by PTH (Fig. 1*H* and *SI Appendix*, Fig. S1*H*). In contrast, sequestration of cell surface Gβγ by masGRK3ct had minimal effect on cAMP responses measured in HEK-$G_{q/11}^{KO}$ cells (*SI Appendix*, Fig. S4 *A* and *B*). We reasoned that $G_{q/11}$ activation, via provision of Gβγ subunits, may promote assembly of signaling complexes at the cell surface comprised of receptor, βarr, and Gβγ that have previously been reported as key components of PTHR-mediated endosomal cAMP production (12). Indeed, time-course experiments measuring

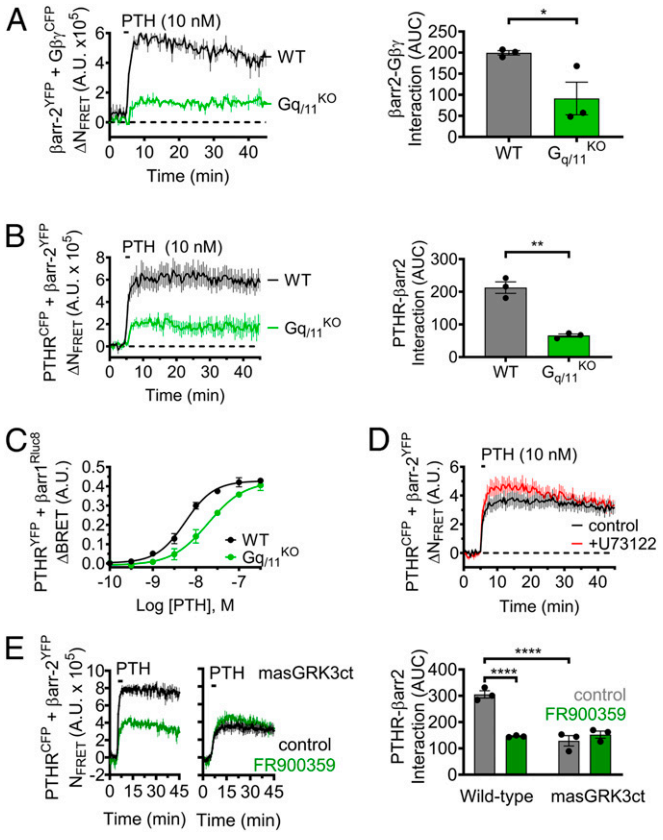

Fig. 2. Effect of $G_{q/11}$ activation on the formation of PTHR endosomal signaling complexes. (*A* and *B*) Time-course experiments measuring FRET between βarr-2^{YFP} and either $G\beta\gamma^{CFP}$ (*A*) or $PTHR^{CFP}$ (*B*) in response to 10 nM PTH in wild-type (WT) HEK293 cells or cells lacking $G\alpha_{q/11}$ ($G_{q/11}^{KO}$). Data represent the mean value ± SEM of n = 3 experiments and n = 17 to 31 cells per experiment (*P < 0.05; **P < 0.01). (*C*) Recruitment of βarr to the PTHR as a function of PTH concentration measured by BRET in cells cotransfected with βarr-1^{Rluc8} and $PTHR^{YFP}$. Data represent the mean ± SEM of n = 3 experiments. (*D*) Similar experiments as in *B* with the PLC inhibitor U73122. Data represent the mean value ± SEM of n = 3 experiments and n = 23 to 30 cells per experiment. (*E*) Effect of masGRK3ct on βarr recruitment to the receptor upon exposure to 10 nM PTH ±FR900359 in cells transfected with $PTHR^{CFP}$ and βarr-2^{YFP}. Data represent the mean value ± SEM of n = 3 experiments and n = 16 to 18 cells per experiment (****P < 0.0001).

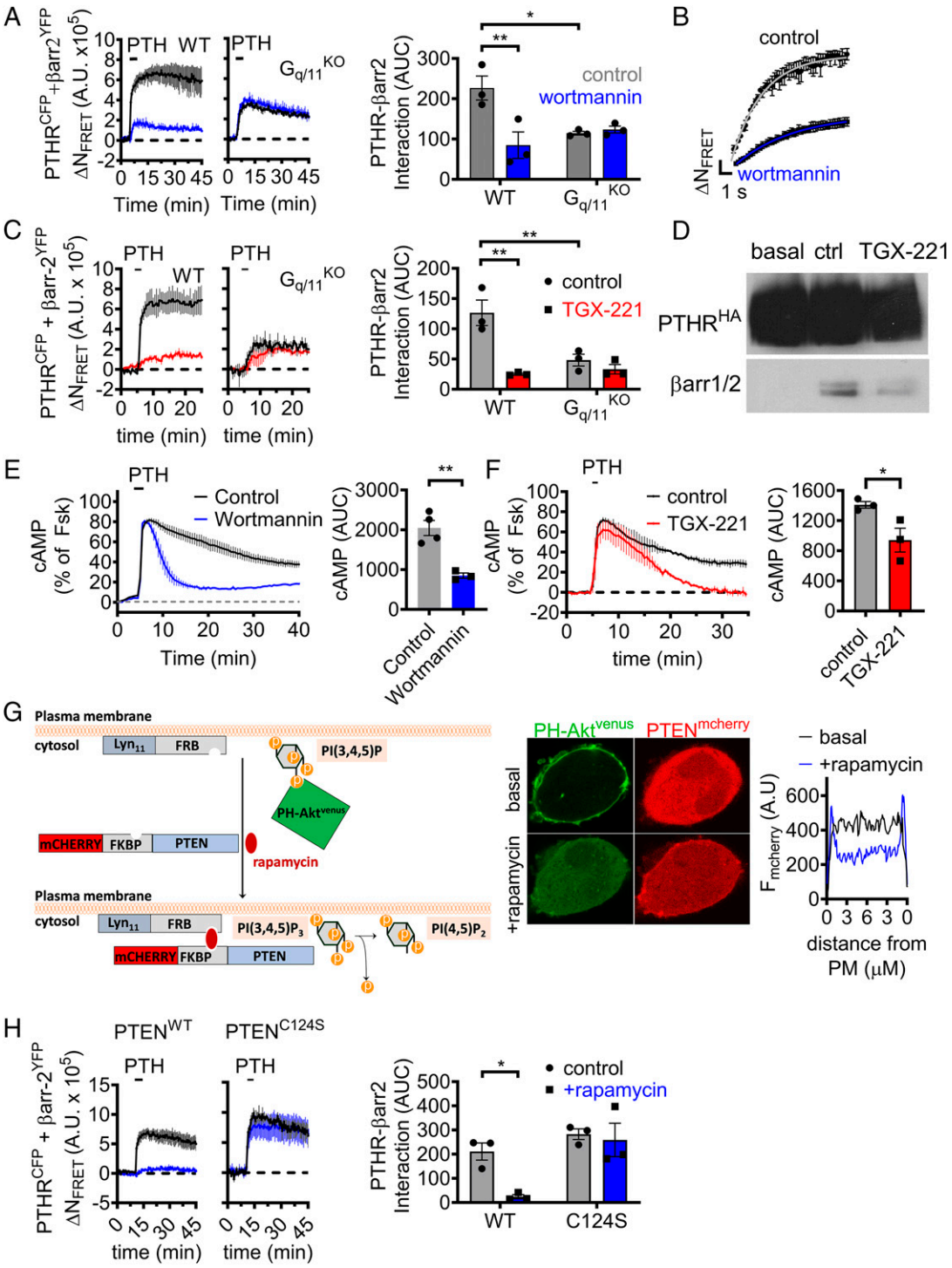

Fig. 3. Recruitment of βarr is regulated by $G_{q/11}$-dependent activation of PI3Kβ. (*A* and *B*) Time-course experiments measuring FRET between βarr-2^{YFP} and PTHR^{CFP} in response to 10 nM PTH ± the PI3K inhibitor wortmannin in wild-type (WT) HEK293 cells or cells lacking $G\alpha_{q/11}$ ($G_{q/11}{}^{KO}$) and kinetics corresponding to experiments shown for WT with rate constant t = 2.5 ± 0.2 s (control) and t = 4.9 ± 0.2 s for wortmannin (*B*). Data represent the mean value ± SEM of $n = 3$ experiments and $n = 20$ to 23 cells per experiment (*$P < 0.05$; **$P < 0.01$). (*C*) Similar experiments as in *A*, using the selective PI3Kβ inhibitor TGX-221. Data represent the mean value ± SEM of $n = 3$ experiments and $n = 7$ to 23 cells per experiment (**$P < 0.01$). (*D*) Interaction between PTHR and βarr detected by coimmunoprecipitation assay. HEK293 cells stably expressing HA-PTHR were preincubated with TGX-221 for 30 min and then stimulated with 100 nM PTH for 5 min. PTHR–βarr complexes were pulled down using anti-HA antibody. (*E* and *F*) Averaged cAMP responses in HEK293 cells stably expressing PTHR following brief exposure to 1 nM PTH ± wortmannin (*E*) or TGX-221 (*F*). Data represent the mean value ± SEM of $n = 3$ to 4 experiments and $n = 15$ to 37 cells for (*E*) and $n = 13$ to 32 cells (*F*) per experiment (*$P < 0.05$; **$P < 0.01$). (*G*) Schematic of rapamycin induced recruitment of PTEN to the plasma membrane that causes acute depletion of PtdIns(3,4,5)P_3 (*Left*) and the efficacy of this system in HEK293 cells transiently expressing FKBP-PTEN^{mcherry}, Lyn_{11}-FRB, and the PIP_3 probe PH-Akt^{venus} (*Center*). To illustrate the specific location of mcherry-PTEN, histograms were drawn representing transects across cells before (black) and after (blue) addition of rapamycin (*Right*). (*H*) Time-course experiments measuring FRET between βarr-2^{YFP} and PTHR^{CFP} in response to 10 nM PTH ± rapamycin in cells coexpressing Lyn_{11}-FRB and either FKBP-tagged wild-type PTEN (PTEN^{WT}) or a catalytically dead mutant (PTEN^{C124S}). Data represent the mean value ± SEM of $n = 3$ experiments and $n = 14$ to 29 cells (PTEN^{WT}) and $n = 12$ to 24 cells (PTEN^{C124S}) per experiment (*$P < 0.05$).

FRET between βarr-2^{YFP} and either Gβγ^{CFP} or PTHR^{CFP} in response to PTH in single cells showed significantly impaired interactions in HEK-$G_{q/11}{}^{KO}$ cells compared with the parental cell line (Fig. 2 *A* and *B*). The unexpected effect of $G_{q/11}$ activation on βarr recruitment was confirmed in subsequent multiplate Bioluminescence Resonance Energy Transfer (BRET)-based assays using PTHR^{YFP} and βarr-1^{Rluc8}, which showed reduced potency (EC_{50}) of PTH-induced recruitment of βarr in HEK-$G_{q/11}{}^{KO}$ (19.2 ± 0.44 nM) compared with parental cells (6.95 ± 0.44 nM; Fig. 2*C*). Consistent with data obtained for cAMP responses, additional FRET recordings showed that the reduced interaction between PTHR and βarr is not due to lack of PLC activity (Fig. 2*D*), but rather the availability of liberated Gβγ subunits at the cell surface derived from heterotrimeric $G_{q/11}$ proteins (Fig. 2*E*).

We subsequently sought to elucidate the mechanistic basis by which $G_{q/11}$-derived Gβγ subunits promote βarr recruitment to the PTHR. The well-established ability of Gβγ to activate GPCR kinases (GRKs) 2/3, coupled to previous reports that phosphorylation of activated GPCRs at serine/threonine residues within the receptor's third intracellular loop (ICL3) and C-terminal tail regulates βarr recruitment (13), led us to examine PTHR phosphorylation status in response to PTH. To this end, we performed stable isotope labeling by amino acids in cell culture (SILAC)-based quantitative phosphoproteomic analysis via liquid chromatography coupled to tandem mass spectrometry (LC-MS-MS). Comparison of wild-type versus $G_{q/11}{}^{KO}$ cells revealed no significant differences in phosphorylation sites nor the extent of phosphorylation (*SI Appendix*, Figs. S5 and S6 and Table S1). These data suggest that $G_{q/11}$-mediated alterations in PTHR–βarr interactions occur in a manner that is independent of receptor phosphorylation.

In addition to GRK2/3, Gβγ subunits have been shown to activate class I phosphoinositide 3-kinases (PI3K). Specifically, PI3Kβ and PI3Kγ isoforms are recruited to the plasma membrane by liberated Gβγ subunits and catalyze the conversion of phosphatidylinositol-(4,5)diphosphate [PtdIns(4,5)P_2] to PtdIns(3,4,5)P_3 (14). Given the previously reported enhanced binding affinity of βarrs for PtdIns(3,4,5)P_3 compared with PtdIns(4,5)P_2 (15), we hypothesized that $G_{q/11}$-dependent activation of class I PI3K and generation of PtdIns(3,4,5)P_3 at the cell surface may promote translocation of βarr to the PTHR. We tested this possibility using the PI3K inhibitor wortmannin in time-course experiments, measuring βarr recruitment by FRET between PTHR^{CFP} and βarr-2^{YFP} in response to PTH. Indeed, we observed significantly slower kinetics and decreased magnitude of βarr-2 association with the receptor in wild-type HEK293 cells preincubated with wortmannin compared with control cells (Fig. 3 *A* and *B*); however, this effect was completely abolished in analogous experiments performed in HEK-$G_{q/11}{}^{KO}$ (Fig. 3*A*). Due to the relative nonselectivity of wortmannin, we repeated these experiments using the PI3Kβ-specific inhibitor TGX-221 (16), which similarly reduced βarr recruitment to the PTHR in wild-type but not $G_{q/11}{}^{KO}$ cells (Fig. 3*C*). Furthermore, the effect of TGX-221 on PTHR–βarr interactions in wild-type cells was confirmed by coimmunoprecipitation assays (Fig. 3*D*). Consistent with a role in endosomal signaling, wortmannin and TGX-221 also markedly reduced the duration of PTH-induced cAMP responses in wild-type cells (Fig. 3 *E* and *F*). The role of PI3K was further confirmed by assessing its direct activation by Gβγ, using the interfering small molecule inhibitor gallein, which has previously been reported to block interaction between Gβγ and class I PI3K (17). As expected, HEK-PTHR cells treated with gallein showed markedly impaired sustained cAMP signaling (*SI Appendix*, Fig. S4*C*). Altogether, these results provide evidence that $G_{q/11}$-dependent PI3Kβ activation via Gβγ represents a major mechanism for both the kinetics and magnitude of βarr interaction to the PTHR, which, in turn, regulates endosomal cAMP signaling.

In addition to its lipid kinase function, PI3Kβ also has been shown to phosphorylate effector proteins (18). To differentiate lipid versus protein kinase actions of PI3Kβ in mediating βarr recruitment, we utilized chemically induced dimerization between FK506 binding protein 12 (FKBP) and the FKBP12 rapamycin binding (FRB) domain of mTOR (19) to recruit PTEN to the plasma membrane. PTEN is a lipid phosphatase that dephosphorylates predominantly PtdIns(3,4,5)P_3, but also PtdIns(3,4)P_2 to some extent, at the 3′ position (20). By expressing mcherry-tagged PTEN-FKBP and FRB fused to the plasma membrane-targeting sequence Lyn_{11}, addition of rapamycin results in acute depletion of PtdIns(3,4,5)P_3 specifically at the plasma membrane (Fig. 3 *G*, *Left*). We confirmed the efficacy of this approach using confocal imaging with cells coexpressing PTEN-FKBP-mcherry, Lyn_{11}-FRB, and the venus-conjugated PH domain from Akt (PH-Akt-venus) that binds selectively the 3′-phosphate in PtdIns(3,4,5)P_3 (20). Under basal conditions, PH-Akt-venus

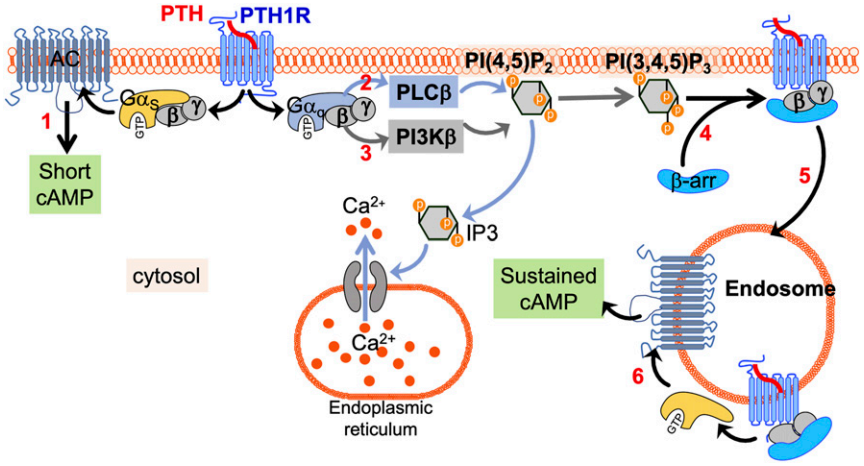

Fig. 4. Proposed model underlying $G_{q/11}$-mediated enhancement of PTHR endosomal cAMP. Binding of PTH to the PTHR results in activation of heterotrimeric Gs and Gq proteins at the cell surface, resulting in stimulation of adenylyl cyclase (*1*) and $PLC_β$ (*2*) via $Gα_S$ and $Gα_q$, respectively. In addition, liberation of Gβγ subunits specifically from $Gα_q$ promotes $PI3K_β$-dependent generation of PI(3,4,5)P_3 (*3*), which subsequently facilitates βarr recruitment to the PTHR (*4*) and formation of ternary PTHR–βarr–Gβγ complexes that remain active following translocation from the cell surface to early endosomes (*5*), and thus permit a sustained phase of cAMP production (*6*).

localized almost exclusively at the plasma membrane, but rapidly translocated to the cytoplasm upon addition of rapamycin (Fig. 3 *G*, *Middle* and *Right*). In contrast, expression of a catalytically dead mutant of PTEN ($PTEN^{C124S}$) (21) did not affect the cellular localization of PH-Akt-venus (*SI Appendix*, Fig. S7). We subsequently used this system in FRET-based time courses of βarr recruitment, which revealed a significant reduction in PTHR–βarr interactions in the presence of rapamycin in cells expressing wild-type PTEN ($PTEN^{WT}$), but not in those expressing $PTEN^{C124S}$ (Fig. 3*H*). Taken together, these findings suggest that $G_{q/11}$-dependent generation of PtdIns(3,4,5)P_3 by PI3Kβ at the plasma membrane serves as a critical regulator of βarr recruitment to the PTHR, and thus the propensity of the receptor to engage in endosomal cAMP signaling in response to PTH.

Discussion

Initially thought to induce signaling exclusively from the plasma membrane, several GPCRs are now recognized for eliciting responses from intracellular compartments, including the Golgi apparatus (22) and endosomes (5). Notably, studies involving the class B PTHR have shown that binding of PTH causes sustained cAMP responses attributed to ligand–receptor complexes that remain active in early endosomes following βarr-mediated internalization (4, 5, 7, 12). Accordingly, endosomal cAMP responses are thus considered to be regulated by G_s- and βarr-dependent signaling pathways (12). While the PTHR also activates $G_{q/11}$ in response to PTH, the role of this pathway in endosomal cAMP generation has been ignored because of its foremost association with the PLC/Ca^{2+} pathway. Mechanistically, our findings unveil that $G_{q/11}$ promotes PI3Kβ-mediated generation of PtdIns(3,4,5)P_3 (PIP_3) at the plasma membrane, and that this represents a critical determinant for association of βarr with the PTHR (Fig. 4). Further understanding of how PIP_3 can be used to promote the association between arrestin and PTHR will require, for example, structural studies to determine whether PIP_3 directly binds to the PTHR to stabilize a functional active state that favors formation of the PTHR–arrestin complex. Another question to be explored is whether the PIP_3-dependent recruitment of arrestin is restricted to either the PTHR or receptors with G_s/G_q signaling pleiotropy, such as class B GPCRs. This is particularly pertinent, given that PIP_3 was previously reported to have no effect on βarr recruitment to the class A β_2-adrenergic receptor (β_2AR) (23). Thus, future investigations into other receptors that couple to G_q and engage in sustained cAMP signaling from intracellular compartments may provide insight into the breadth of PtdIns(3,4,5)P_3-mediated regulation of GPCR–βarr interactions. Collectively, our findings identify a regulatory mechanism of PTH-induced cAMP, wherein $G_{q/11}$-derived Gβγ subunits enhance the assembly of ternary PTHR–βarr–Gβγ complexes at the cell surface, which permits endosomal cAMP generation. While previous studies have implicated Gβγ-dependent modulation of adenylyl cyclase activity in the context of receptor functional crosstalk (24), our results provide an instance of a single GPCR that uses $G_{q/11}$-dependent formation of signaling complexes to control the spatial organization and duration of G_s-mediated cAMP production.

Materials and Methods

Cell Culture and Transfection. Cell culture reagents were obtained from Corning (CellGro). Human embryonic kidney cells (HEK293; ATCC, Washington, DC) stably expressing the recombinant human PTHR were grown in DMEM containing 5% FBS and 1% penicillin/streptomycin at 37 °C in a humidified atmosphere containing 5% CO_2. Primary mouse calvarial osteoblast (Ob) cells were isolated and cultured as described (24); RPTEC were grown in DMEM/F12 supplemented with 5 PM triiodo-L-thyronine, 10 ng/mL recombinant human epidermal growth factor, 25 ng/mL prostaglandin E1, 3.5 μg/mL ascorbic acid, 1 mg/mL insulin, 0.55 mg/mL transferrin, 0.5 μg/mL sodium selenite, 25 ng/mL hydrocortisone plus 1% penicillin and streptomycin. For transient expression, cells were seeded on glass coverslips coated with poly-D-lysine in six-well plates and cultured for 24 h prior transfection with plasmids using Lipofectamine 3000 (Life Technologies) for 48 h before experiments. Optimized amounts of plasmids were determined based on the specific assay and to ensure fluorescent intensities that were readily detectable yet not saturating.

Peptides and Chemicals. PTH(1–34), the N-terminal synthetic analog of naturally circulating PTH(1–84), and TMR-labeled PTH(1–34) were generated as previously described (25). Forskolin (#344270) was purchased from EMD-Millipore. FR900359 (known as UBO-QIC former commercial name) was extracted from Ardisia crenata following a previously published protocol (26).

Plasmids. DNA constructs encoding for $PTHR^{YFP}$, $PTHR^{CFP}$, and βarr-2^{YFP} were previously described by Vilardaga laboratory (4, 27, 28). βarr-1^{Rluc8} was provided by Zachary Freyberg, University of Pittsburgh; $G\alpha_q{}^{YFP}$, $G\beta_1$BiFc (Cer[1-158]-$G\beta_1$), and $G\gamma_2$BiFc (CFP[159-238]-$G\gamma_2$) were a gift from Catherine Berlot, Weis Center for Research, Geisinger Clinic, Danville, PA, and can be found in Addgene (#66081, #55782, #55707, and #55707, respectively); Gα11 was a gift from Tom Gardella, MGH; masGRK3ct was a kind gift from Nevin Lambert, Augusta University; and FKBPPTEN and FRB-Lyn_{11} were provided by Gerry Hammon, University of Pittsburgh.

Western Blot of Endogenous $G_{q/11}$ Expression. Total protein extracts were prepared using cell lysis buffer (1% Nonidet P-40, 1% sodium deoxycholate, 0.1% SDS, 50 mM Tris at pH 7.4, 150 mM NaCl, 1 mM EDTA, $NaVO_3$) containing EDTA-free Protease Inhibitor Mixture (Roche Diagnostic GmbH). Proteins were quantified by the Micro BCA protein assay kit (Thermo Fisher scientific #23225) according to the manufacturer's instructions. Proteins were separated on a 10% SDS/PAGE and transferred to a nitrocellulose membrane. Membranes were blocked for 1 h in TBS/0.1% Tween20 containing 5% nonfat milk supplemented by 1% BSA. Membrane was incubated overnight with a mouse anti-$G_{q/11}$ antibody (Santa Cruz Biotechnologies, #365906) followed by incubation with HRP-conjugated polyclonal goat anti-mouse antibody (Dako). For loading control, membrane was reprobed with anti-b-tubulin antibody (Thermo Fisher, #MA5-16308) following stripping (10% SDS, 0.5 M Tris at pH 6.8, 0.8% β-Mercaptoethanol).

Coimmunoprecipitation. HEK293 cells stably expressing HA-PTHR and cultured on a 10-cm dish were preincubated with serum-free DMEM ± 100 nM TGX-221 and then stimulated with 100 nM PTH for 5 min. Cells were then washed with ice-cold PBS before 2 h incubation with 1 mM cross-linkerDSP (Covachem, #13301) at 4 °C. Crosslinking was neutralized upon treatment with 10 mM Tris·HCl for 10 min, followed by lysing of cells with buffer containing 1% Triton X-100, 50 mM Tris·HCl at pH 7.4, 140 mM NaCl, 0.5 mM EDTA, protease and phosphatase inhibitors (Roche, #11873580001). BCA protein assay kits (Thermo Fisher, #23225) were utilized to quantify protein concentration, and lysates were subsequently incubated overnight at 4 °C in the presence of anti-HA antibody-coated agarose beads (Sigma Aldrich, #A2095; clone HA7). To elute bound proteins, we incubated beads with LDS loading buffer (Life Technologies) and then loaded samples on 10% SDS/PAGE and transferred to nitrocellulose membrane. Antibodies against HA (Covance, clone 16B12) and βarr-1/2 (Cell Signaling; #4674, clone D24H9) were utilized to detect receptor and βarr, respectively. Immunoreactive bands were visualized with Luminata Forte (EMD Millipore) and autoradiography film.

Time-Course Measurements of cAMP Production and βarr Recruitment in Live Cells. cAMP was assessed using FRET-based assays. Cells were transiently transfected with the FRET-based biosensor, $Epac1^{CFP/YFP}$ (29), for measuring cAMP. Measurements were performed and analyzed as previously described (25). In brief, cells plated on poly-D-lysine coated glass coverslips were mounted in Attofluor cell chambers (Life Technologies), maintained in Hepes buffer containing 150 mM NaCl, 20 mM Hepes, 2.5 mM KCl, 1 mM $CaCl_2$, and 0.1% BSA at pH 7.4, and cell chambers were placed on the oil immersion 40× N.A 1.30 Plan Apo objective of our Nikon Ti-E microscope (Nikon Corporation). To measure cAMP responses (intramolecular FRET) and recruitment of βarr (intermolecular FRET), CFP was excited using a mercury lamp. Emissions for CFP and YFP were filtered using a 480 ± 20 and 535 ± 15 nm, respectively. Intensities were collected with a LUCAS EMCCD camera (Andor), utilizing a DualView 2 (Photometric) with a beam splitter dichroic long pass of 505 nm. To calculate FRET ratios, individual fluorophore intensities were obtained from individual cells using Nikon Element Software (Nikon), and ratios were calculated as we have shown previously (30).

Saturation and Competition Binding at Equilibrium. HEK293 cells were transiently transfected with HA-PTHR and seeded in 96-well plates. Approximately 48 h after transfection, cells were incubated in Hepes buffer (137 mM NaCl/5 mM KCl/1 mM $MgCl_2$/1 mM $CaCl_2$/20 mM Hepes/0.1% BSA at pH 7.4) for 1 h at 4 °C, followed by 2 h incubation at 4 °C in the presence of ligand. Increasing concentration of TMR-labeled PTH (PTH^{TMR}) were utilized for saturation binding, while competition binding experiments used a constant PTH^{TMR} concentration (31.6 nM) with increasing amounts of unlabeled PTH. Cells were washed twice with the same buffer, and fluorescence intensities were recorded at 580 ± 20 nm using an excitation wavelength of 525 ± 20 nm on a Tecan Spark 20M multimode microplate reader. Nonspecific binding was determined using 1 μM unlabeled ligand. Data were subsequently analyzed using GraphPad Prism 7.0 (GraphPad Software Inc.).

Laser Scanning Confocal Microscopy. Cells plated on coverslips were mounted in Attofluor cell chambers (Life Technologies) and incubated with Hepes buffer containing 150 mM NaCl, 20 mM Hepes, 2.5 mM KCl, 1 mM $CaCl_2$, and 0.1% BSA at pH 7.4, and transferred on the Nikon Ti-E microscope (Nikon) equipped with a Z-driven piezo motor. Imaging was performed using Nikon A1 confocal unit, through a 60× N.A. = 1.45 objective (Nikon). Fluorescent proteins or peptides were excited with 440-nm (CFP or Turquoise), 514-nm (YFP), or 561-nm (TMR) lasers (Melles Griot). Data acquisitions were performed using Nikon Element Software (Nikon Corporation). After acquisition, raw data were analyzed using ImageJ software. Each different analysis was performed at the single-cell level.

BRET Recording of PTHR–βarr Interaction. HEK293 cells were transiently transfected with βarr-1^{Rluc8} and $PTHR^{YFP}$ and seeded in 96-well plates. Approximately 48 h after transfection, cells were incubated in Hepes buffer (137 mM NaCl/5 mM KCl/1 mM $MgCl_2$/1 mM $CaCl_2$/20 mM Hepes/0.1% BSA at pH 7.4) at 37 °C in the presence of 5 μM coelenterazine-h for 10 min, followed by addition of increasing concentrations of PTH. Donor and acceptor luminescence (466 and 535 nm, respectively) were measured at 2.5-min intervals using a Tecan Spark 20M multiplate reader. For each well, the maximum luminescence observed, which typically occurred 10 min after PTH stimulation, was utilized to calculate BRET ratios (acceptor/donor). Data were subsequently analyzed using GraphPad Prism 7.0 (GraphPad Software) and expressed as ΔBRET, which was determined by subtracting ratios obtained in control wells containing cells with donor alone.

Statistical Analysis. Data were processed using Excel 2013 (Microsoft Corp.) and Prism 7.0 (GraphPad Software Inc.). Data are expressed as mean ± SEM. Curves were fit to the data using a four-parameter, nonlinear regression function. Statistical analyses were performed using unpaired, two-tailed Student's *t* tests for comparisons between two groups.

Data Availability. Materials will be made available to all qualified investigators with a simple institutional material transfer agreement. Data and associated protocols will be provided upon reasonable request.

ACKNOWLEDGMENTS. Research reported in this publication was supported by the National Institute of Diabetes and Digestive and Kidney Disease and the National Institute of General Medical Sciences of the National Institutes of Health under Grant Awards Numbers R01-DK111427, R01-DK116780, and R01-DK122259 (to J.-P.V.), and R01-GM056414 (to S.H.G.). J.-P.V. thanks Nevin Lambert (Augusta University) for providing the MasGRK3ct construct and Gerry Hammond (University of Pittsburgh) for providing the FKBP-PTEN and FRB-Lyn_{11} constructs.

1. H. Jüppner *et al*., A G protein-linked receptor for parathyroid hormone and parathyroid hormone-related peptide. *Science* **254**, 1024–1026 (1991).
2. J. T. Potts, H. M. Kronenberg, M. Rosenblatt, "Parathyroid hormone: Chemistry, biosynthesis, and mode of action" in *Advances in Protein Chemistry*, C. B. Anfinsen, J. T. Edsall, Eds. (Academic Press, Richards, FM, 1982), vol. 35, pp. 323–396.
3. A. B. Abou-Samra *et al*., Expression cloning of a common receptor for parathyroid hormone and parathyroid hormone-related peptide from rat osteoblast-like cells: A single receptor stimulates intracellular accumulation of both cAMP and inositol trisphosphates and increases intracellular free calcium. *Proc. Natl. Acad. Sci. U.S.A.* **89**, 2732–2736 (1992).
4. S. Ferrandon *et al*., Sustained cyclic AMP production by parathyroid hormone receptor endocytosis. *Nat. Chem. Biol.* **5**, 734–742 (2009).
5. J. P. Vilardaga, F. G. Jean-Alphonse, T. J. Gardella, Endosomal generation of cAMP in GPCR signaling. *Nat. Chem. Biol.* **10**, 700–706 (2014).
6. S. Lee *et al*., A homozygous [Cys25]PTH(1-84) mutation that impairs PTH/PTHrP receptor activation defines a novel form of hypoparathyroidism. *J. Bone Miner. Res.* **30**, 1803–1813 (2015).
7. A. D. White *et al*., Ca^{2+} allostery in PTH-receptor signaling. *Proc. Natl. Acad. Sci. U.S.A.* **116**, 3294–3299 (2019).
8. M. Okazaki *et al*., Prolonged signaling at the parathyroid hormone receptor by peptide ligands targeted to a specific receptor conformation. *Proc. Natl. Acad. Sci. U.S.A.* **105**, 16525–16530 (2008).
9. I. Sutkeviciute, L. J. Clark, A. D. White, T. J. Gardella, J. P. Vilardaga, PTH/PTHrP receptor signaling, allostery, and structures. *Trends Endocrinol. Metab.* **30**, 860–874 (2019).
10. S. Liu *et al*., Use of backbone modification to enlarge the spatiotemporal diversity of parathyroid hormone receptor-1 signaling via biased agonism. *J. Am. Chem. Soc.* **141**, 14486–14490 (2019).
11. B. Hollins, S. Kuravi, G. J. Digby, N. A. Lambert, The c-terminus of GRK3 indicates rapid dissociation of G protein heterotrimers. *Cell. Signal.* **21**, 1015–1021 (2009).
12. V. L. Wehbi *et al*., Noncanonical GPCR signaling arising from a PTH receptor-arrestin-Gβγ complex. *Proc. Natl. Acad. Sci. U.S.A.* **110**, 1530–1535 (2013).
13. D. Mayer *et al*., Distinct G protein-coupled receptor phosphorylation motifs modulate arrestin affinity and activation and global conformation. *Nat. Commun.* **10**, 1261 (2019).
14. H. Kurosu *et al*., Heterodimeric phosphoinositide 3-kinase consisting of p85 and p110beta is synergistically activated by the betagamma subunits of G proteins and phosphotyrosyl peptide. *J. Biol. Chem.* **272**, 24252–24256 (1997).
15. I. Gaidarov, J. G. Krupnick, J. R. Falck, J. L. Benovic, J. H. Keen, Arrestin function in G protein-coupled receptor endocytosis requires phosphoinositide binding. *EMBO J.* **18**, 871–881 (1999).
16. S. P. Jackson *et al*., PI 3-kinase p110beta: A new target for antithrombotic therapy. *Nat. Med.* **11**, 507–514 (2005).
17. D. M. Lehmann, A. M. Seneviratne, A. V. Smrcka, Small molecule disruption of G protein beta gamma subunit signaling inhibits neutrophil chemotaxis and inflammation. *Mol. Pharmacol.* **73**, 410–418 (2008).
18. D. Thomas *et al*., Protein kinase activity of phosphoinositide 3-kinase regulates cytokine-dependent cell survival. *PLoS Biol.* **11**, e1001515 (2013).
19. P. J. Belshaw, S. N. Ho, G. R. Crabtree, S. L. Schreiber, Controlling protein association and subcellular localization with a synthetic ligand that induces heterodimerization of proteins. *Proc. Natl. Acad. Sci. U.S.A.* **93**, 4604–4607 (1996).
20. B. D. Goulden *et al*., A high-avidity biosensor reveals plasma membrane $PI(3,4)P_2$ is predominantly a class I PI3K signaling product. *J. Cell Biol.* **218**, 1066–1079 (2019).
21. M. P. Myers *et al*., P-TEN, the tumor suppressor from human chromosome 10q23, is a dual-specificity phosphatase. *Proc. Natl. Acad. Sci. U.S.A.* **94**, 9052–9057 (1997).
22. R. Irannejad *et al*., Functional selectivity of GPCR-directed drug action through location bias. *Nat. Chem. Biol.* **13**, 799–806 (2017).
23. S. V. Naga Prasad *et al*., Phosphoinositide 3-kinase regulates beta2-adrenergic receptor endocytosis by AP-2 recruitment to the receptor/beta-arrestin complex. *J. Cell Biol.* **158**, 563–575 (2002).
24. F. G. Jean-Alphonse *et al*., β_2-adrenergic receptor control of endosomal PTH receptor signaling via Gβγ. *Nat. Chem. Biol.* **13**, 259–261 (2017).
25. A. Gidon, T. N. Feinstein, K. Xiao, J. P. Vilardaga, Studying the regulation of endosomal cAMP production in GPCR signaling. *Methods Cell Biol.* **132**, 109–126 (2016).
26. R. Schrage *et al*., The experimental power of FR900359 to study Gq-regulated biological processes. *Nat. Commun.* **6**, 10156 (2015).
27. J. P. Vilardaga, M. Bünemann, C. Krasel, M. Castro, M. J. Lohse, Measurement of the millisecond activation switch of G protein-coupled receptors in living cells. *Nat. Biotechnol.* **21**, 807–812 (2003).
28. T. N. Feinstein *et al*., Retromer terminates the generation of cAMP by internalized PTH receptors. *Nat. Chem. Biol.* **7**, 278–284 (2011).
29. V. O. Nikolaev, M. Bünemann, L. Hein, A. Hannawacker, M. J. Lohse, Novel single chain cAMP sensors for receptor-induced signal propagation. *J. Biol. Chem.* **279**, 37215–37218 (2004).
30. J. P. Vilardaga, Studying ligand efficacy at G protein-coupled receptors using FRET. *Methods Mol. Biol.* **756**, 133–148 (2011).